atmosphere

MDPI

Article

Vertical Profiles of Atmospheric Species Concentrations and Nighttime Boundary Layer Structure in the Dry Season over an Urban Environment in Central Amazon Collected by an Unmanned Aerial Vehicle

Patrícia Guimarães [1,2], Jianhuai Ye [3], Carla Batista [1,2], Rafael Barbosa [1,2], Igor Ribeiro [1,2], Adan Medeiros [2], Tianning Zhao [3], Wei-Chun Hwang [4], Hui-Ming Hung [4], Rodrigo Souza [2] and Scot T. Martin [3,5,*]

1 Post-Graduate Program in Climate and Environment, National Institute of Amazonian Research and Amazonas State University, Manaus, Amazonas 69060-001, Brazil; guimaraespc.uea@gmail.com (P.G.); cestefanibatista@gmail.com (C.B.); rgb.barbosa@gmail.com (R.B.); igorgeoinformacao@gmail.com (I.R.)
2 School of Technology, Amazonas State University, Manaus, Amazonas 69065-020, Brazil; adan_medeiros@hotmail.com (A.M.); souzaraf@gmail.com (R.S.)
3 School of Engineering and Applied Sciences, Harvard University, Cambridge, MA 02138, USA; jye@seas.harvard.edu (J.Y.); zhaot@g.harvard.edu (T.Z.)
4 Department of Atmospheric Sciences, National Taiwan University No. 1, Sec. 4, Roosevelt Road, Taipei 10617, Taiwan; r06229008@ntu.edu.tw (W.-C.H.); hmhung@ntu.edu.tw (H.-M.H.)
5 School of Engineering and Applied Sciences and Department of Earth and Planetary Sciences, Harvard University, Cambridge, MA 02138, USA
* Correspondence: scot_martin@harvard.edu

Received: 27 October 2020; Accepted: 23 November 2020; Published: 18 December 2020

Abstract: Nighttime vertical profiles of ozone, $PM_{2.5}$ and PM_{10} particulate matter, carbon monoxide, temperature, and humidity were collected by a copter-type unmanned aerial vehicle (UAV) over the city of Manaus, Brazil, in central Amazon during the dry season of 2018. The vertical profiles were analyzed to understand the structure of the urban nighttime boundary layer (NBL) and pollution within it. The ozone concentration, temperature, and humidity had an inflection between 225 and 350 m on most nights, representing the top of the urban NBL. The profile of carbon monoxide concentration correlated well with the local evening vehicular congestion of a modern transportation fleet, providing insight into the surface-atmosphere dynamics. In contrast, events of elevated $PM_{2.5}$ and PM_{10} concentrations were not explained well by local urban emissions, but rather by back trajectories that intersected regional biomass burning. These results highlight the potential of the emerging technologies of sensor payloads on UAVs to provide new constraints and insights for understanding the pollution dynamics in nighttime boundary layers in urban regions.

Keywords: air pollution; central Amazon; nighttime; dry season; ozone; boundary layer; unmanned aerial vehicle

1. Introduction

In 1985 and 1987, the Amazon Boundary Layer Experiment (ABLE) provided important characterization of the structure of the atmospheric boundary layer in the Amazon region [1–4]. The ABLE focus was for the daytime, and less attention was given to the nighttime boundary layer (NBL). Investigations of the NBL in the Amazon are scarce, and the previous studies largely focused

on the NBL over forest and pasture [5–9]. For the wet season, Guimarães et al. [10] reported on the NBL over an urban environment in the Amazon and found significant differences compared to the NBL over forests and pastures.

Santos [8] and Neves and Fisch [7] expressed the great importance, yet challenge, in studying the NBL and identifying its vertical structure. There are difficulties in describing and modeling the processes that define the NBL structure, such as processes that suppress or increase turbulence. To first order, radiative effects at night lead to the development of a temperature inversion in the atmospheric profile Stull [11]. Under ideal circumstances, this inversion is associated with calm conditions and little turbulence, and an isolated near-surface air mass called the nighttime boundary layer forms. The height and structure of the NBL are best identified under clear skies and over homogeneous terrain. Compared to the ideal scenario, moderate to strong winds above the NBL can induce shearing turbulence in the otherwise quiescent NBL and disrupt its structure in complex ways [5]. Atmospheric movements, such as gravity waves associated with heterogeneous terrains, can coexist with turbulence and can further complicate the structure of the NBL. These complex interacting effects warrant the collection of datasets for better understanding the NBL.

Seasonality is one important factor that affects the NBL in the Amazon. The extent and rate of nighttime cooling directly affects the height of the NBL. In the wet season compared to the dry season, less longwave radiative cooling occurs at night because there is more low-level cloudiness and there is greater absolute humidity in the overlying atmosphere [9,12]. Less cooling weakens the overhead temperature inversion, and the NBL is usually shallower and less stable in the wet season compared with the dry season. Thus, the study of the NBL in both seasons is important for understanding the NBL over urban landscapes, where factors such as anthropogenic emissions and radiative effects which reinforce the effects of heat islands, are not experienced over forest and pasture landscapes.

Another under-investigated factor is the urban environment. Cities cover a small percentage of land area, but are home to a large part of the human population, especially in the Amazon. Compared with forested regions, the urban landscape absorbs more heat during the day. Land surface permeability to water is also reduced so that evapotranspiration is substantially altered. These changes in the surface boundary conditions can strongly influence the structure of the overhead NBL. Moreover, the local roughness of houses and buildings is substantially different from that of the forest canopy, and interactions and propagation of shearing turbulence and injection can also strongly differ. As a result, whereas the average NBL heights in the Amazon are typically 150–280 m and 210–230 m during the wet season for forest and pasture environments, respectively [9,10], that NBL heights are higher and approach 300 m for the urban environment in the wet season. The higher NBL heights occur because the intensity of turbulence increases over the urban region in response to the altered physical parameters, as discussed above [13–16].

Corsmeier et al. [17], Aneja et al. [18], Salmond and McKendry [19] for different worldwide locations and Guimarães et al. [10] for Amazonia showed the possibility of using the vertical structure of ozone concentration to study and characterize the NBL. The ozone concentration in a fair-weather day in Amazonia follows a well-established cycle [20,21]. Ozone is produced by photochemical processes throughout the day, starting with sunrise. In the absence of pollution, emissions of nitric oxide (NO) from tropical soils and volatile organic compounds (VOCs) from the tropical forest are important precursors to the photochemical reactions throughout Amazonia [22,23]. Subsequently, after sunset and throughout the night, the ozone concentration strongly decreases because atmospheric production falls off and dry deposition processes to the land surface dominate. The ozone concentration near Earth's surface can drop below the detection level of commonly employed instruments.

This nighttime ozone behavior means that vertical profiles of ozone concentration can be used to investigate the NBL structure [10]. During conditions of atmospheric stability, the temperature inversion capping the NBL isolates ozone in the surface region from ozone at higher altitudes. Ozone deposition to surface and atmospheric reactions with NO decrease ozone concentration in this isolated air mass. Any occurrence of relatively high ozone concentrations in the vertical structure of the air mass thus

implicates the occurrence of ozone intrusions from higher altitudes and reveals the structure of the NBL, including possible turbulent injections. In addition to ozone concentration, other gaseous or particulate pollutants, such as carbon dioxide, methane, nitrogen oxides, and aerosol particles, can be used as tracers for NBL height and structure depending on local factors of emission and loss of these species [24–30].

For the wet season, Guimarães et al. [10] reported results of the nighttime boundary layer over an urban region. Ozone sensors equipped to an unmanned aerial vehicle (UAV) were used for data collection. The UAV platform enabled data collection with temporal and spatial resolution in the vertical structure [31–37]. In addition to the classic structure reviewed by Stull [11], Guimarães et al. [10] reported two additional classes of atmospheric profiles that largely correlated with nighttime cloud cover.

In this paper, results from flights in the dry season are presented, and differences between the two seasons were analyzed. Moreover, compared with Guimarães et al. [10] for which ozone concentration, temperature, and relative humidity were collected, a broader range of species concentrations was collected in this study. Profiles of carbon monoxide and particulate matter ($PM_{2.5}$ and PM_{10}) were simultaneously collected. These species are markers of urban pollution and biomass burning, both of which can have continuous nighttime surface sources. By comparison, ozone derives from an overhead reservoir that undergoes dry deposition at the surface throughout the night. Thus, process-wise, the two sets of species strongly complement one another.

2. Experiment

A hexacopter UAV (DJI Matrice 600 Professional Grade, Figure S4) was used for the measurements. A description of the UAV platform is presented in Guimarães et al. [10]. Briefly, the UAV had maximum flight times of 35 min without payload and 25 min with mounted instrumentation (0.5–1.0 kg). The maximum ascending and descending speeds were 5 and 3 m s^{-1}, respectively. Geofencing by the manufacturer limited flight height to 500 m above local ground. The UAV was equipped with Global Positioning System (GPS). Latitude, longitude, altitude, and flight speed were recorded during flights.

UAV flights were performed on the campus of the School of Technology at the Amazonas State University (3.0918° S, 60.0175° W). The campus is centrally located in Manaus. The campus is surrounded by a forested region that transitions into urbanized residential and commercial areas surrounding the campus (Figure 1). Manaus is the largest and most populous city in Amazonas state in Brazil. It has more than 2 million residents, and its urbanized land area is more than 200 km^2.

During flights, the concentration of ozone was measured onboard the UAV. A commercial ozone sensor (Personal Ozone Monitor, 2B Technologies Inc., Boulder, CO, USA) was positioned on the top platform of the UAV. Over the course of the campaign, regular sensor calibration was carried out (Model 306, 2B Technologies Inc.). The detection limit of the sensor was 3 ppbv (2-sigma variation). The sensor measurement had an accuracy of the greater of 2 ppbv or 2% of the reading. The sampling flow rate to the sensor was 0.8 L min^{-1}, and the concentration was measured every 10 s. Temperature and pressure were measured redundantly by this sensor and an additional one (HOBO U12 Series). A GPS module embedded in the sensor continuously recorded latitude, longitude, altitude, and time. This dataset provided a redundancy check to telemetry of the UAV navigation module. For data analysis, the ozone concentrations measured by the sensor were binned and averaged for every vertical interval of 15 m from the ground level up to a height of 500 m.

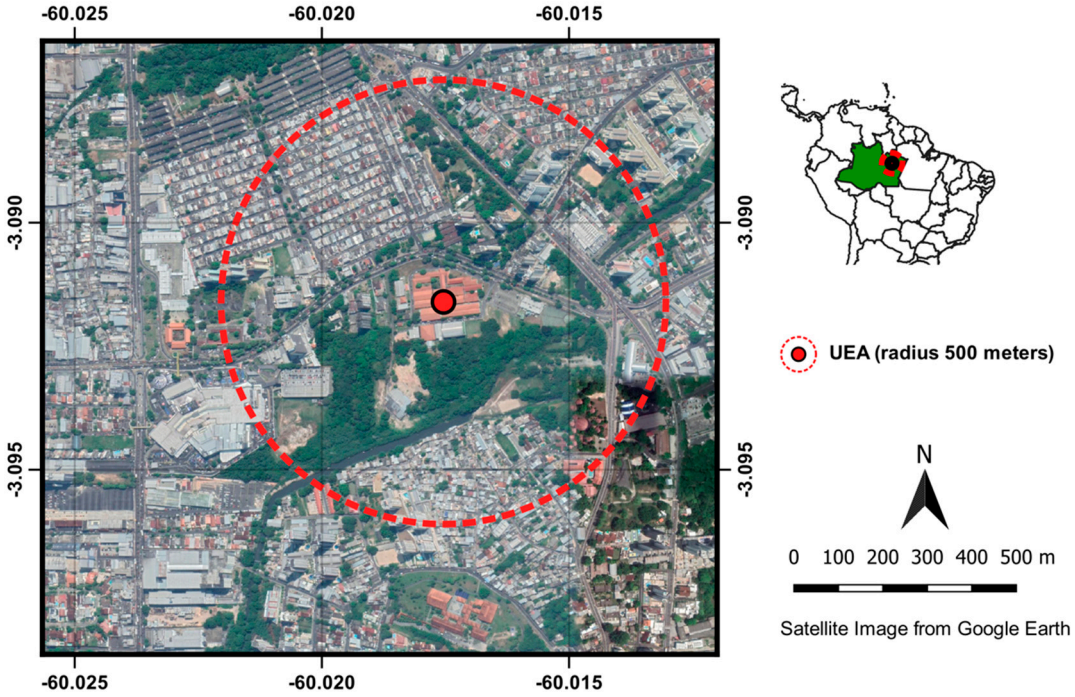

Figure 1. Representative image of the study area in the city of Manaus, Brazil, in central Amazon. The urban region is crossed by rivers and interspersed with forests. Nighttime flights to collect vertical profiles took place on the campus of the Amazonas State University (marked as a red disc and labeled "UEA") in the middle of the city. The green region in the inset shows the state of Amazonas, Brazil, in South America.

A laboratory-built sensor package was affixed to the bottom platform of the UAV. The sensor package measured concentrations of CO, CO_2, SO_2, $PM_{2.5}$, and PM_{10} as well as temperature, relative humidity, and atmospheric pressure. The trace gases were detected by electrochemical sensors with ppbv detection sensitivity from Alphasense (Essex, UK). The particulate matter was characterized by an optical particle counter (OPC-N2, Alphasense). The sensor package operated and recorded the data every second. The sensors were calibrated at the National Taiwan University before and after the measurement campaign. After each UAV flight, the onboard sensor package was referenced to an identical package on the ground to ensure that the onboard sensors did not drift and functioned consistently.

The UAV flights were performed during the dry season from 13 September 2018 to 13 October 2018. During the study period, flights took place on 12 nights. On a typical night, eight flights were carried out every 30 min from 20:00 to 00:00 (local time (LT)). LT was 4 h earlier than Coordinated Universal Time (UTC). For each flight, the ascending speed was 0.5 m s^{-1}, which minimized the influence of local turbulence and mixing from the UAV propellers [35,38]. In total, there were 84 flights, (Table S1), and the ozone sensor was active on all flights. The CO, CO_2, SO_2, $PM_{2.5}$, and PM_{10} sensor package worked properly during 32 of these flights (4 nights).

In complement to the measurements, an atmospheric chemistry/transport model, called *Lagrangian Integrated Trajectory of Single Particles HYbrid* (HYSPLIT, version 4), was used in the analysis [39,40]. The objective was to simulate back trajectories at the point of UAV sampling to identify possible pollutant sources. The simulations were carried out for the near-surface layer from 0 to 500 m and back trajectories to 12 h. Biomass burning was identified from the *Suomi*-NPP satellite at a spatial resolution of 375 m [41]. The land use map from *MapBiomas* was used [42].

3. Results and Discussion

Observations of nighttime ozone concentration recorded by the UAV flights at different altitudes at the urban UEA campus in central Amazon are presented in Figure 2 for the wet and dry seasons. The vertical profiles are individually plotted in Figure S1 for each night. The data for the wet season were from Guimarães et al. [10] (Figure 2a), and the statistics of those observations were re-plotted in this study for comparison between the two seasons. The work of Guimarães et al. [10] was conducted at the same location and times of night as the present study. The data of the dry season of this study are plotted in Figure 2b.

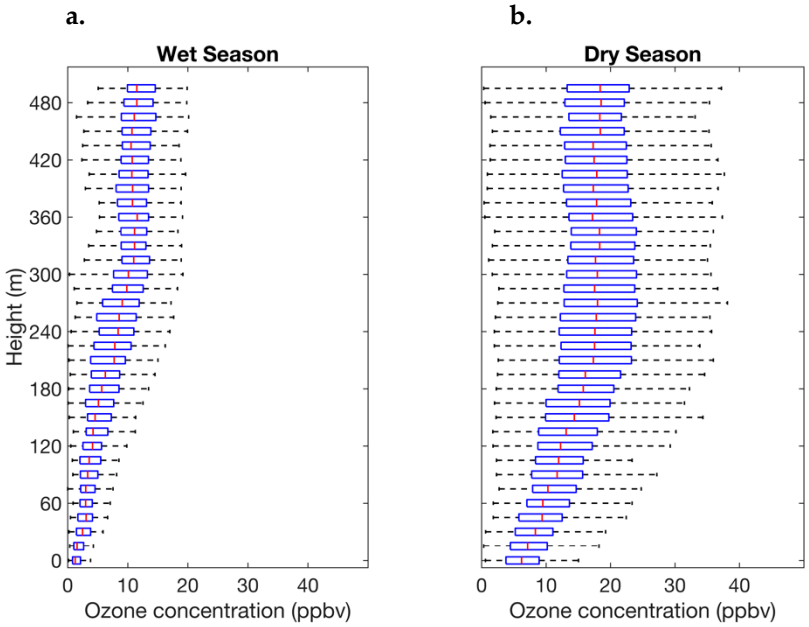

Figure 2. Box-whisker plots of the statistics of ozone concentration at different altitudes. Results are presented for the (**a**) wet and (**b**) dry seasons of 2018 (57 and 84 flights, respectively). The red line represents the median, the box edges show the quartiles, and the horizontal black lines indicate the minimum and maximum values, excluding outliers. Flights took place between 20:00 and 00:00 (local time (LT)). LT was 4 h earlier than UTC. The data of panel (**a**) are from Guimarães et al. [10].

The profiles of ozone concentration in the wet and dry seasons could be compared. The median of the ozone concentration close to the surface was <3 ppbv in the wet season, while in the dry season it was 6 ppbv. The median at the top of the NBL of 10 ppbv in the wet season doubled to 20 ppbv in the dry season. Likewise, the maximum concentration at the top of the NBL doubled from 20 ppbv in the wet season to 40 ppbv in the dry season. These differences are connected to the seasonality of ozone concentrations in the region [20]. Ozone is produced by photochemical cycles that involve sunlight, VOCs, and NO_x [23]. In the dry season, the large-scale convective systems shift northward from most of Amazonia [43], leading to less cloud cover and greater solar irradiation [44,45]. Besides directly stimulating ozone production through more rapid photochemistry, greater solar radiation also enhances VOC emissions from the forest. In addition, there is an intensification of burning activities in the region that releases NO_x [18]. All of these factors tend to increase ozone concentrations in the dry season. Even so, for both seasons, there is a decline of ozone concentration in the vertical profile from the top of the NBL to the land surface, and hence ozone is a good proxy for characterization of the NBL in both seasons.

The NBL height was determined in part based on the profiles of ozone concentration, potential temperature, and relative humidity using the method presented in Guimarães et al. [10]. Inflection points in the profiles represent the top of the NBL. There is typically a steep slope of the increasing ozone concentration and relative humidity at the inflection point. Potential temperature

can sometimes behave similarly, although there are more exceptions because of the urban heat island (see below). In addition, compared to Guimarães et al. [10], the present study had additional chemical information, and this information was also used to confirm the NBL height.

Figure 3 shows the box-whisker statistics plots of the height of the nighttime boundary layer during the dry season based on 84 flights. Whereas the average NBL heights in the Amazon are typically 180–330 m and 120–230 m during the dry season for forest and pasture environments, respectively [9], Figure 3 shows that the typical NBL heights approached 225–350 m for the urban environment in the dry season. As discussed in Guimarães et al. [10], the higher NBL heights can be related to the effects of the urban heat island. A high heat capacity of the urban canopy leads to increased accumulation of solar energy during the day. Moreover, reduced evapotranspiration because of landcover changes reduces cooling mechanisms relative to the forest. These combined factors intensify daytime heating of the surface and retain temperature through the night. The nighttime profile of potential temperature in some cases can be complicated by these factors, leading to uncertainties in estimates of the NBL height by potential temperature. By comparison, estimates of the NBL height by ozone concentration are not affected by the urban heat island, thus demonstrating the usefulness of this chemical proxy for characterizing the NBL.

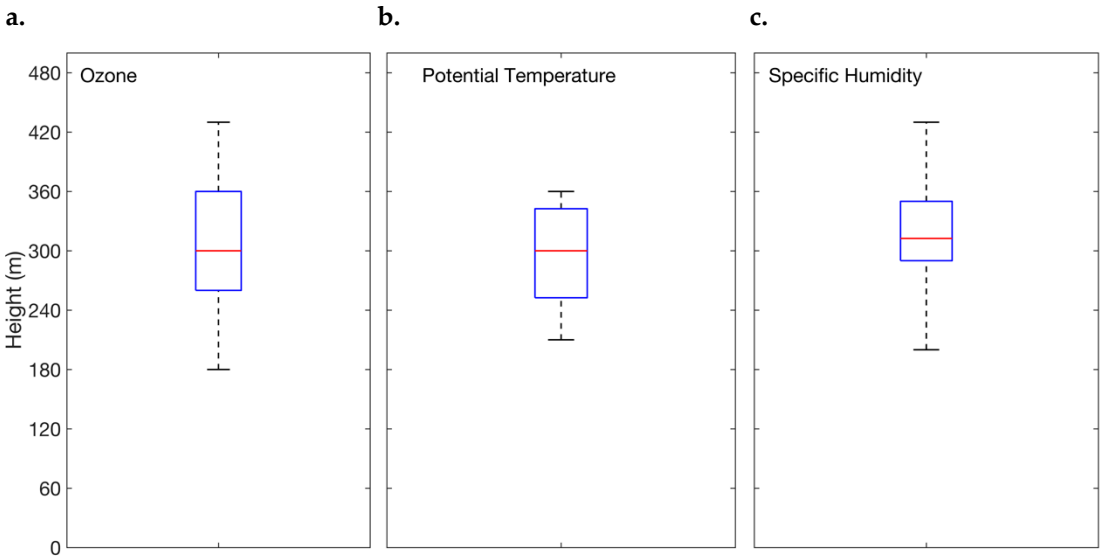

Figure 3. Box-whisker statistics plots of the height of the nighttime boundary layer during the dry season of 2018 based on (**a**) ozone concentration, (**b**) potential temperature, and (**c**) specific humidity (84 flights). The median (red line), quartiles (blue box edges), and the minimum and maximum values (black lines) are represented, excluding outliers. Flights took place between 20:00 and 00:00 (LT). Local time (LT) was 4 h earlier than UTC.

The CO, $PM_{2.5}$, and PM_{10} pollution sensors on the UAV provided an additional perspective on the structure of the nighttime boundary layer. Figure 4 plots examples of eight vertical profiles collected on the night of 29 September 2018. The profiles extended from land surface to an altitude of 500 m. The red line represents the median of the data at each altitude. The vertical profile of ozone concentration is well explained by entrainment of ozone-laden air above the NBL height and its dry deposition to the land surface, as described above. By comparison, the vertical profile of carbon monoxide has a different behavior. A typical background concentration for Amazonia is 80–120 ppbv [21]. The observed surface concentration on 29 September 2018 was 500 ppbv. The explanation for higher concentrations is CO emission from the urban vehicular fleet [46,47]. The concentration decreases to the regional background concentration of 100 ppbv by 200 m. The profiles of O_3 and CO concentrations are thus the inverse of one another. Ozone has an overhead regional source and a surface sink, and carbon monoxide has a localized urban surface source that dilutes to the regional background concentration at altitude.

The profiles are symmetric by a mirror plane, and both profiles separately indicated an NBL height on this night of 160–200 m, which was lower than typical during the study period (see above). A step profile in concentration is characteristic of quiescent nights [10]. By comparison, the gently sloped profiles of O_3 and CO concentration in Figure 4 indicated a night of moderate downward injection and turbulence. In this regard, the two independent profiles provided a consistent conclusion. The vertical profiles of $PM_{2.5}$ and PM_{10} plotted in Figure 4 indicated an absence of significant local pollution on this night. The consumer vehicular fleet active during nighttime congestion in Manaus is modern, and the direct emissions of $PM_{2.5}$ and PM_{10} from this fleet are small (the daytime fleet includes heavy vehicles that emit soot from diesel engines).

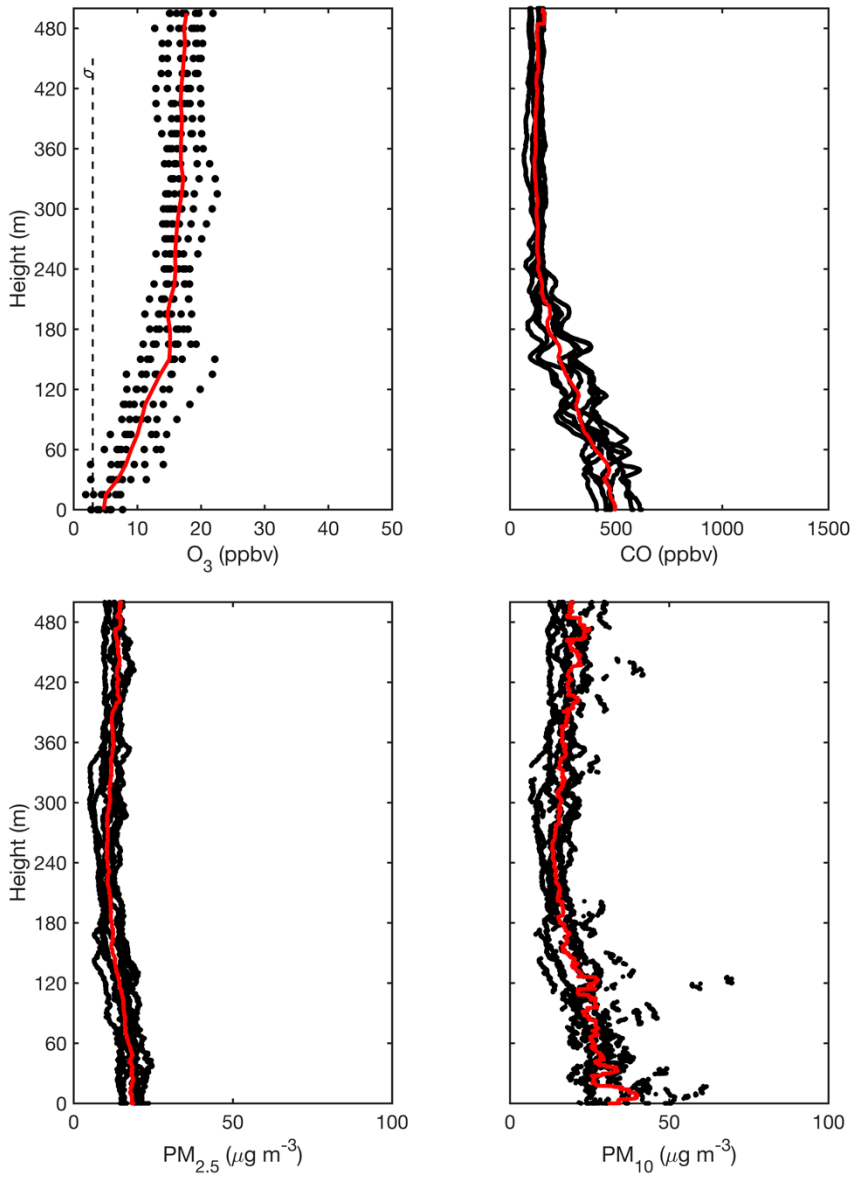

Figure 4. Vertical profiles of the concentrations of ozone, carbon monoxide, $PM_{2.5}$, and PM_{10} from land surface to an altitude of 500 m for 8 flights on 29 September 2018 between 20:00 and 00:00 (LT). The red line represents the median of the data at each altitude. The dashed line represents the instrumental limit of detection for ozone (3 ppbv). Individual profiles are plotted in Figure S2.

Figure 5 plots vertical profiles of the same type as Figure 4 but for a different night on 27 September 2018. The symmetric relation by mirror plane between the vertical profiles of O_3 and CO concentrations was again apparent (Figure 5). Compared with Figure 4, the NBL transition was more abrupt.

This observation indicated a more quiescent night with little turbulent intrusion. In addition, there was a clear increase of NBL height over time. The NBL height increased from 150–170 m at 20:00 to 230–250 m at 21:00, and further to 270–280 m at 22:00. Across time, the vertical profiles evolved through replacement of one species with another. The three species, meaning ozone, CO, and PM, have largely independent sources, and thus each profile leads to an independently supported conclusion, and the overall conclusion can thus be regarded as thricely supported. This linked behavior and conclusion demonstrated the important capability of the UAV-based chemical sensing to probe the evolution and dynamics of the atmospheric boundary layer.

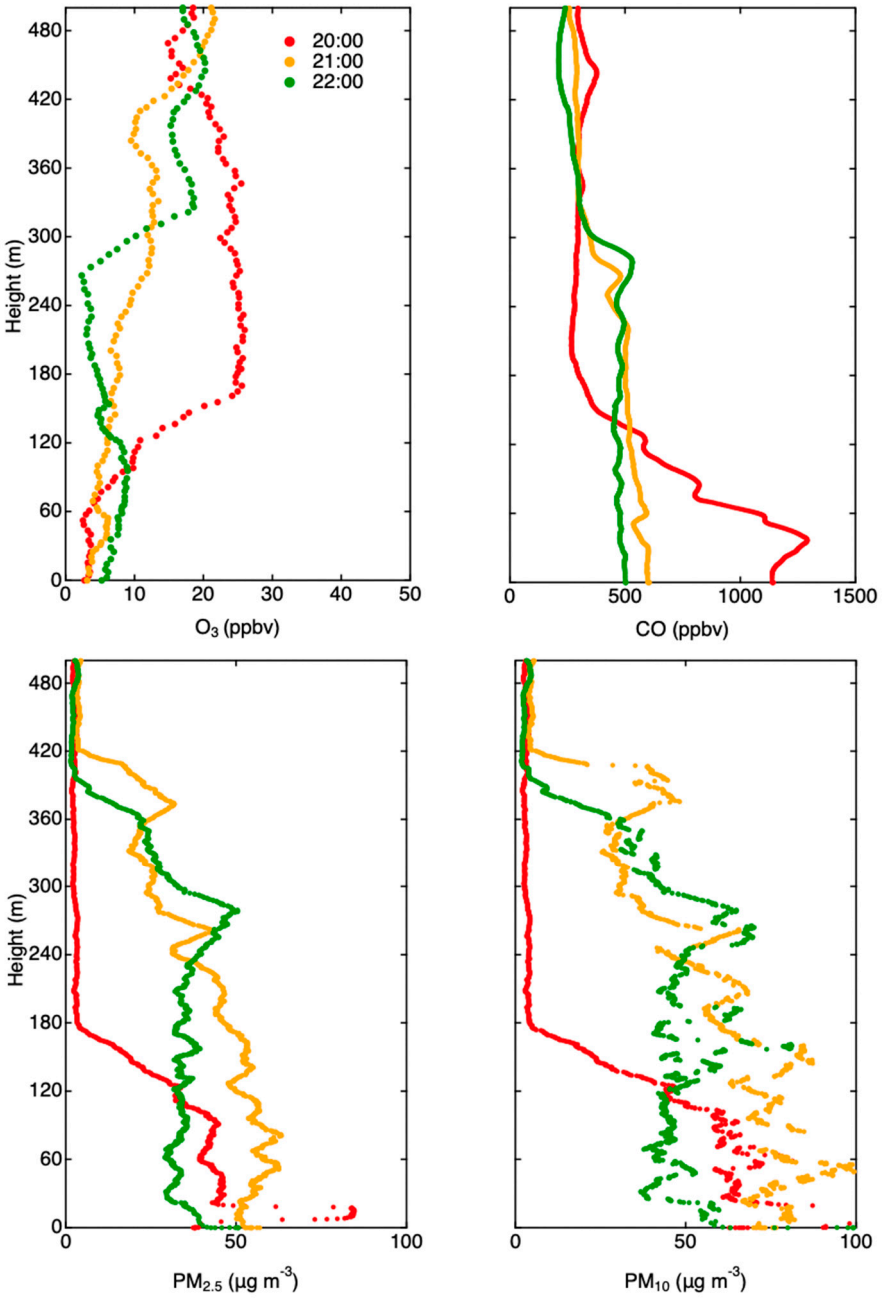

Figure 5. Evolution of vertical profiles of the concentrations of ozone, carbon monoxide, $PM_{2.5}$, and PM_{10} from land surface to an altitude of 500 m on 27 September 2018 from 20:00 to 22:00 (LT).

There were several other differences between the two nights. The CO concentration was >1000 ppbv on 27 September 2018, which was more than double its value on 29 September 2018. Moreover, the vertical profiles of $PM_{2.5}$ and PM_{10} concentrations differed strongly from one another

between the two nights. On 29 September 2018, the vertical profiles of PM concentrations had little structure and provided no direct information about the NBL. On 27 September 2018, there was a high PM concentration near the surface. The implication was that the PM concentration and the elevated CO concentration came from a different source than the vehicular fleet. This source appeared to be biomass burning.

The HYSPLIT model was used to simulate atmospheric back trajectories for the near-surface layer from 0 to 500 m at the heights and times of UAV sampling corresponding to Figures 4 and 5 (Figure S3). For 29 September 2018, the 12-h back trajectories were northeasterlies across the forest and a relatively few vicinal fires. For 27 September 2018, the back trajectories were southeasterlies across a farming region characterized by many fire spots. The back trajectories were consistent with the effect of regional biomass burning emissions as the explanation for the differences in the $PM_{2.5}$ and PM_{10} concentrations between Figures 4 and 5. The vertical profiles collected by the UAV indicated that this regional pollution stayed tightly contained within the NBL across the trajectory distance of tens of kilometers.

4. Conclusions

The results of this study highlighted the potential of the emerging technologies of sensor payloads on UAVs to provide new constraints and insights for understanding the pollution dynamics in nighttime boundary layers in urban regions. This study demonstrated the powerful efficacy of three different tracers from three different sources for mapping out the structure of the NBL. These tracers included regional ozone descending to the surface from overhead entrainment, carbon monoxide from transportation and biomass burning surface emissions, and particulate matter from long-distance Amazonian biomass burning. These datasets serve as new constraints that can test and improve high-resolution environmental models of NBL structure.

Supplementary Materials: The following are available online at http://www.mdpi.com/2073-4433/11/12/1371/s1. Table S1: Flight count on each night. Figure S1: Vertical profiles of ozone concentration, potential temperature, and specific humidity. Figure S2: Vertical profiles of concentrations of carbon dioxide, carbon monoxide, sulfur dioxide, $PM_{2.5}$, and PM_{10}. Figure S3: Back trajectories at UAV sampling point for altitudes of 0, 100, 200, 300, 400, and 500 m. Figure S4: Photograph of the hexacopter UAV equipped with sensor package.

Author Contributions: Conceptualization, S.T.M., P.G., R.B.; methodology, P.G., S.T.M.; software, P.G., I.R., A.M.; validation, P.G., J.Y., T.Z., W.-C.H., H.-M.H.; formal analysis, P.G., I.R.; investigation, P.G., C.B., R.B.; resources, S.T.M., R.S., P.G.; data curation, P.G., J.Y.; writing—original draft preparation, P.G., S.T.M.; writing—review and editing, P.G., T.Z., W.-C.H., H.-M.H., J.Y., S.T.M.; visualization, P.G., J.Y.; supervision, S.T.M., R.S.; project administration, P.G.; funding acquisition, S.T.M., R.S. All authors have read and agreed to the published version of the manuscript.

Funding: The authors from Brazil acknowledge funding by the Brazilian Federal Agency for Support and Evaluation of Graduate Education (CAPES) (88881.187481/2018-01) and the Brazilian National Council for Scientific and Technological Development (CNPq) (142166/2015-4). The authors from the USA acknowledge funding from the Harvard Climate Change Solutions Fund, the Postdoctoral Program in Environmental Chemistry of the Dreyfus Foundation, and the Division of Atmospheric and Geospace Sciences of the USA National Science Foundation (AGS-1829025). The Brazilian Air Force, through the Department of Airspace Control (DECEA) and the National Civil Aviation Agency (ANAC), provided flight authorizations and other support for the measurements. The flight operations followed the regulatory norms of ANAC and associated agencies (RBAC-E No. 94/2017).

Conflicts of Interest: The authors declare no conflict of interest.

Data Availability: The vertical profiles of concentrations of ozone, particulate matter, and carbon monoxide as well as temperature and humidity recorded during the campaign are available (https://doi.org/10.7910/DVN/QUYO2D).

References

1. Garstang, M.; Fitzjarrald, D.R. *Observations of Surface to Atmosphere Interactions in the Tropics*; Oxford University Press: Oxford, UK, 1999.
2. Harriss, R.C.; Wofsy, S.C.; Garstang, M.; Browell, E.V.; Molion, L.C.B.; McNeal, R.J.; Hoell, J.M.; Bendura, R.J.; Beck, S.M.; Navarro, R.L.; et al. The Amazon Boundary Layer Experiment (ABLE 2A): Dry season 1985. *J. Geophys. Res. Space Phys.* **1988**, *93*, 1351. [CrossRef]

3. Kirchhoff, V.W.J.H.; Rasmussen, R.A. Time variations of CO and O_3 concentrations in a region subject to biomass burning. *J. Geophys. Res. Space Phys.* **1990**, *95*, 7521. [CrossRef]
4. Martin, C.L.; Fitzjarrald, D.; Garstang, M.; Oliveira, A.P.; Greco, S.; Browell, E. Structure and growth of the mixing layer over the Amazonian rain forest. *J. Geophys. Res. Space Phys.* **1988**, *93*, 1361. [CrossRef]
5. Carneiro, R.G.; Henkes, A.; Fisch, G.; Borges, C.K. Study of the daily cycle of the planetary boundary layer during the rainy season in the Amazon (GOAMAZON 2014/15). *Sci. Nat.* **2018**, *40*, 63–68.
6. Fisch, G. Camada Limite Amazônica: Aspectos Observacionais e de Modelagem (Amazonian Boundary Lyer: Observations and Modeling). Ph.D. Thesis, Instituto Nacional de Pesquisas Espaciais (National Institute for Space Research), São José dos Campos, Brazil, December 1995.
7. Neves, T.T.D.A.T.; Fisch, G. Night limit layer on pasture area in the Amazon. *Rev. Bras. Meteorol.* **2011**, *26*, 619–628. [CrossRef]
8. Santos, R.D.; Fisch, G.; Dolman, A.; Waterloo, M. Modelagem da Camada Limite Noturna (CLN) durante a época úmida na Amazônia, sob diferentes condições de desenvolvimento. *Rev. Bras. Meteorol.* **2007**, *22*, 387–407. [CrossRef]
9. Santos, R.M.N. Nighttime Boundary Layer Studies in the Amazon. Ph.D. Thesis, Instituto Nacional de Pesquisas Espaciais (National Institute for Space Research), Sao Jose dos Campos, Brazil, 2005.
10. Guimarães, P.; Ye, J.; Batista, C.; Barbosa, R.; Ribeiro, I.; Medeiros, A.; Souza, R.; Martin, S.T. Vertical profiles of Ozone concentration collected by an Unmanned Aerial Vehicle and the mixing of the Nighttime Boundary Layer over an Amazonian Urban Area. *Atmosphere* **2019**, *10*, 599. [CrossRef]
11. Stull, R.B. *An Introduction to Boundary Mayer Meteorology*; Kluwer: Dordrecht, The Netherlands, 1988.
12. Betts, A.; Fisch, G.; von Randow, C.; Dias, M.S.; Cohen, J.; da Silva, R.; Fitzjarrald, D. *The Amazon Boundary Layer and Mesoscale Circulations in Amazonia and Global Change*; American Geophysical Union: Washington, DC, USA, 2009.
13. Arya, P.S. *Introduction to Micrometeorology*, 2nd ed.; Academic Press: Cambridge, MA, USA, 2001.
14. Barlow, J.F.; Halios, C.H.; Lane, S.E.; Wood, C.R. Observations of urban boundary layer structure during a strong urban heat island event. *Environ. Fluid Mech.* **2015**, *15*, 373–398. [CrossRef]
15. Oke, T. *Boundary Layer Climates*, 2nd ed.; University Press: Cambridge, MA, USA, 1987; p. 435.
16. Sánchez, M.P.; de Oliveira, A.P.; Valdés, J.T.; Codato, G.; Varona, R.P.; Marques Filho, E.P.; Dutra Ribeiro, F.N.; Rocha Pereira, M.M. Observational Investigation of the Nocturnal Low-Level Jet in the Metropolitan Region of São Paulo. 2017. Available online: http://repositorio.geotech.cu/ (accessed on 12 October 2020).
17. Corsmeier, U.; Kalthoff, N.; Kolle, O.; Kotzian, M.; Fiedler, F. Ozone concentration jump in the stable nocturnal boundary layer during a LLJ-event. *Atmos. Environ.* **1997**, *31*, 1977–1989. [CrossRef]
18. Aneja, V.P.; Mathur, R.; Arya, S.P.; Li, Y.; Murray, G.C.; Manuszak, T.L. Coupling the Vertical Distribution of Ozone in the Atmospheric Boundary Layer. *Environ. Sci. Technol.* **2000**, *34*, 2324–2329. [CrossRef]
19. Salmond, J.; McKendry, I. Secondary ozone maxima in a very stable nocturnal boundary layer: Observations from the Lower Fraser Valley, BC. *Atmos. Environ.* **2002**, *36*, 5771–5782. [CrossRef]
20. Martin, S.T.; Artaxo, P.; Machado, L.A.; Manzi, A.O.; Souza, R.A.F.; Schumacher, C.; Wang, J.; Andreae, M.O.; Barbosa, H.M.J.; Fan, J.; et al. Introduction: Observations and Modeling of the Green Ocean Amazon (GoAmazon2014/5). *Atmos. Chem. Phys. Discuss.* **2016**, *16*, 4785–4797. [CrossRef]
21. Martin, S.T.; Andreae, M.O.; Artaxo, P.; Baumgardner, D.; Chen, Q.; Goldstein, A.H.; Guenther, A.; Heald, C.L.; Mayol-Bracero, O.L.; McMurry, P.H.; et al. Sources and properties of Amazonian aerosol particles. *Rev. Geophys.* **2010**, *48*. [CrossRef]
22. Kirchhoff, V.W.J.H.; Browell, E.V.; Gregory, G.L. Ozone measurements in the troposphere of an Amazonian rain forest environment. *J. Geophys. Res. Space Phys.* **1988**, *93*, 15850. [CrossRef]
23. Rummel, U. Turbulent Exchange of Ozone and Nitrogen Oxides between an Amazonian Rain Forest and the Atmosphere. Ph.D. Thesis, University of Bayreuth, Bayreuth, Germany, 2005; p. 264.
24. Chambers, S.D.; Wang, F.; Williams, A.G.; Deng, X.; Zhang, H.; Lonati, G.; Crawford, J.; Griffiths, A.D.; Iannello, A.; Allegrini, I. Quantifying the influences of atmospheric stability on air pollution in Lanzhou, China, using a radon-based stability monitor. *Atmos. Environ.* **2015**, *107*, 233–243. [CrossRef]
25. Dang, R.; Yang, Y.; Hu, X.; Wang, Z.; Zhang, S. A Review of Techniques for Diagnosing the Atmospheric Boundary Layer Height (ABLH) Using Aerosol Lidar Data. *Remote Sens.* **2019**, *11*, 1590. [CrossRef]

26. Gerbig, C.; Körner, S.; Lin, J.C. Vertical mixing in atmospheric tracer transport models: Error characterization and propagation. *Atmos. Chem. Phys. Discuss.* **2008**, *8*, 591–602. [CrossRef]
27. Gibert, F.; Schmidt, M.; Cuesta, J.; Ciais, P.; Ramonet, M.; Xueref, I.; Larmanou, E.; Flamant, P.H. Retrieval of average CO2fluxes by combining in situ CO2measurements and backscatter lidar information. *J. Geophys. Res. Space Phys.* **2007**, *112*. [CrossRef]
28. Janssen, R.H.H.; De Arellano, J.V.-G.; Ganzeveld, L.N.; Kabat, P.; Jimenez, J.L.; Farmer, D.K.; Van Heerwaarden, C.C.; Mammarella, I. Combined effects of surface conditions, boundary layer dynamics and chemistry on diurnal SOA evolution. *Atmos. Chem. Phys. Discuss.* **2012**, *12*, 6827–6843. [CrossRef]
29. Pal, S.; Lee, T.; Phelps, S.; De Wekker, S. Impact of atmospheric boundary layer depth variability and wind reversal on the diurnal variability of aerosol concentration at a valley site. *Sci. Total Environ.* **2014**, *496*, 424–434. [CrossRef]
30. Pal, S.; Patra, A.S.; Ghorai, S.; Sarkar, A.K.; Mahato, V.; Sarkar, S.; Singh, R. Efficient and rapid adsorption characteristics of templating modified guar gum and silica nanocomposite toward removal of toxic reactive blue and Congo red dyes. *Bioresour. Technol.* **2015**, *191*, 291–299. [CrossRef] [PubMed]
31. Alvarado, M.; Gonzalez, F.; Erskine, P.; Cliff, D.; Heuff, D. A Methodology to Monitor Airborne PM10 Dust Particles Using a Small Unmanned Aerial Vehicle. *Sensors* **2017**, *17*, 343. [CrossRef] [PubMed]
32. Aurell, J.; Mitchell, W.; Chirayath, V.; Jonsson, J.; Tabor, D.; Gullett, B. Field determination of multipollutant, open area combustion source emission factors with a hexacopter unmanned aerial vehicle. *Atmos. Environ.* **2017**, *166*, 433–440. [CrossRef]
33. Chen, Q.; Li, X.-B.; Song, R.; Wang, H.-W.; Li, B.; He, H.-D.; Peng, Z.-R. Development and utilization of hexacopter unmanned aerial vehicle platform to characterize vertical distribution of boundary layer ozone in wintertime. *Atmos. Pollut. Res.* **2020**, *11*, 1073–1083. [CrossRef]
34. Chen, Q.; Wang, D.; Li, X.-B.; Li, B.; Song, R.; He, H.-D.; Peng, Z.-R. Vertical Characteristics of Winter Ozone Distribution within the Boundary Layer in Shanghai Based on Hexacopter Unmanned Aerial Vehicle Platform. *Sustainability* **2019**, *11*, 7026. [CrossRef]
35. McKinney, K.A.; Wang, D.; Ye, J.; De Fouchier, J.-B.; Guimarães, P.C.; Batista, C.E.; Souza, R.A.F.; Alves, E.G.; Gu, D.; Guenther, A.B.; et al. A sampler for atmospheric volatile organic compounds by copter unmanned aerial vehicles. *Atmos. Meas. Tech.* **2019**, *12*, 3123–3135. [CrossRef]
36. Villa, T.F.; Salimi, F.; Morton, K.; Morawska, L.; Gonzalez, F. Development and Validation of a UAV Based System for Air Pollution Measurements. *Sensors* **2016**, *16*, 2202. [CrossRef]
37. Pan, J.-S.; Liu, N.; Chu, S.-C. A Hybrid Differential Evolution Algorithm and Its Application in Unmanned Combat Aerial Vehicle Path Planning. *IEEE Access* **2020**, *8*, 17691–17712. [CrossRef]
38. Ma, Y.; Ye, J.; Ribeiro, I.O.; Vilà-Guerau de Arellano, J.; Xin, J.; Martin, S.T. Optimization and representativeness of atmospheric chemical sampling by hovering unmanned aerial vehicles. *Harv. Dataverse* in peer review.
39. Draxler, R.R.; Hess, G. An overview of the HYSPLIT_4 modelling system for trajectories. *Aust. Meteorol. Mag.* **1998**, *47*, 295–308.
40. Stein, A.; Draxler, R.R.; Rolph, G.D.; Stunder, B.J.; Cohen, M.; Ngan, F. NOAA's HYSPLIT atmospheric transport and dispersion modeling system. *Bull. Am. Meteorol. Soc.* **2015**, *96*, 2059–2077. [CrossRef]
41. INPE. 2020. Available online: http://queimadas.dgi.inpe.br/queimadas/portal (accessed on 25 September 2020).
42. Souza, C.M.; Shimbo, J.Z.; Rosa, M.R.; Parente, L.L.; Alencar, A.; Rudorff, B.F.; Hasenack, H.; Matsumoto, M.; Ferreira, L.G.; Souza-Filho, P.W.M.; et al. Reconstructing Three Decades of Land Use and Land Cover Changes in Brazilian Biomes with Landsat Archive and Earth Engine. *Remote Sens.* **2020**, *12*, 2735. [CrossRef]
43. Zilitinkevich, S.S.; Esau, I.N. *Similarity Theory and Calculation of Turbulent Fluxes at the Surface for the Stably Stratified Atmospheric Boundary Layer in Atmospheric Boundary Layers*; Springer: New York, NY, USA, 2007.
44. Fisch, G.; Marengo, J.A.; Nobre, C.A. A general review of the climate in the Amazon. *Acta Amazon.* **1998**, *28*, 101. [CrossRef]
45. Rummel, U.; Ammann, C.; Kirkman, G.A.; Moura, M.A.L.; Foken, T.; Andreae, M.O.; Meixner, F.X. Seasonal variation of ozone deposition to a tropical rain forest in southwest Amazonia. *Atmos. Chem. Phys. Discuss.* **2007**, *7*, 5415–5435. [CrossRef]

46. Medeiros, A.S.; Calderaro, G.; Guimarães, P.; Magalhaes, M.R.; Morais, M.V.B.; Rafee, S.A.A.; Ribeiro, I.O.; Andreoli, R.V.; Martins, J.A.; Martins, L.D.; et al. Power plant fuel switching and air quality in a tropical, forested environment. *Atmos. Chem. Phys.* **2017**, *17*, 8987–8998. [CrossRef]
47. Rafee, S.A.A.; Martins, L.D.; Kawashima, A.B.; Almeida, D.S.; Morais, M.V.B.; Souza, R.V.A.; Oliveira, M.B.L.; Souza, R.A.F.; Medeiros, A.S.S.; Urbina, V.; et al. Contributions of mobile, stationary and biogenic sources to air pollution in the Amazon rainforest: A numerical study with the WRF-Chem model. *Atmos. Chem. Phys. Discuss.* **2017**, *17*, 7977–7995. [CrossRef]